INTRODUCTION OF A NEW CLASS OF HIGH-POWER Y-JUNCTION CIRCULATORS: THE 352MHz/1.5MW TYPE DESIGNED FOR CERN/LEP

S. LENZ, E. PIVIT, W. HAUTH - ANT TELECOMMUNICATIONS

Abstract

This paper presents the design and performance of a new type of high-power waveguide Y-circulator, which was developed and manufactured for the LEP storage ring. The design uses the method of dividing the RF input power into several ferrite-loaded cells. The circulator is capable of handling 1MW CW power at 352MHz with its output shorted at any phase. Operation into a load at the output leads to a typical insertion loss of <0.08dB (including ferrite losses of ≈0.04dB), and a 20dB-bandwidth (reflection and isolation) of 6%.

History of high-power circulator development

Considering high-energy physics, especially particle accelerators, a circulator is an important component in an RF accelerating system because of its decoupling function. If inserted between a high-power transmitter (klystron) and accelerating cavity, the circulator protects sensitive power sources and stabilizes operating conditions due to the decrease of load pulling effects and - consequently - reduces downtime in accelerator systems.
In 1969, the first high-power phase-shift circulator, developed for DESY/Hamburg, was presented [1]. For more than ten years, this type of circulator design - often manufactured by various companies - was the only solution for high-power applications exceeding the 100 kW range. But, because of the large weight, enormous dimensions and high price of such a phase-shift circulator, a new start was attempted with the development of a 500MHz/500kW waveguide Y-junction circulator in the early eighties. Up to that time, this circulator type had been considered as unsuitable for such high power levels for several reasons [2,3]. A successful realization of the required 500kW version [4] (also designed for DESY), however, has provided know-how and confidence to start the development of the CERN/LEP Y-junction circulator.

Design considerations

In the following a brief overview of the thermal and electrical design of the circulator will be given:

- discussion of temperature behaviour of the ferrite resonator in conjunction with its geometry
- field theoretical simulation of the frequency behaviour of the ferrite resonator
- scattering matrix evaluation of the resonator coupled to the waveguide
- transformation of resonator impedance

Thermal design

At high power levels the loss mechanism inside the circulator is the main point to be taken into account. In contrast to a standard low-power design, heating-up of ferrites due to losses is a predominant factor, because temperature gradients may damage the ferrites as well as shift the operating point to non-optimum values. The electrical parameters of the circulator are de-tuned, because the saturation magnetization of a ferrite material depends on temperature. Due to this experience, ferrite temperature rises must be kept as low as possible.

This may be effected by:
- using a low loss-ferrite material (ANT-RG1, H=16 Oe) and operating it in the 'above resonance region'
- splitting the RF power onto several flat ferrite-loaded discs
- cooling the discs to remove dissipation heat from the ferrites.

The temperature difference inside the ferrite material is

$$\Delta T_0 = h_f \cdot P_f \,/\, (2 \cdot \Theta \cdot A) \qquad (1)$$

where h_f = ferrite thickness
P_f = ferrite dissipation loss
Θ = heat-conduction coefficient
A = ferrite disc surface area

Thus, minimizing ΔT_0 means maximizing the surface area while reducing the ferrite height. When bearing in mind that not only the thermal, but also the electrical design has to be optimized, it can be seen that there must be a compromise between the required parameters, which will be discussed at a later stage.

Temperature dependence of ferrite material properties

The non - reciprocal function of a ferrite-loaded junction magnetized perpendicular to the direction of the propagating wave is determined by the permeability (Polder) tensor, with diagonal element μ and off-diagonal element κ. Fig. 1 shows the variation of these two elements versus the external magnetic field strength at two different temperatures.

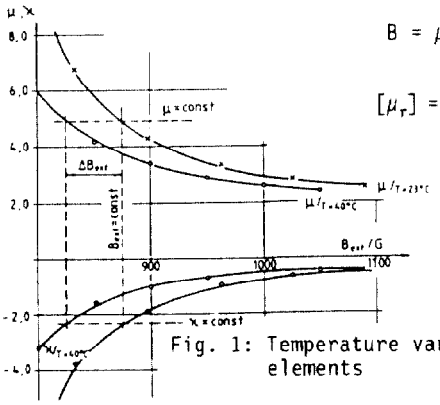

$$B = \mu_0[\mu_r]H$$

$$[\mu_r] = \begin{bmatrix} \mu & -j\kappa & 0 \\ j\kappa & \mu & 0 \\ 0 & 0 & 1 \end{bmatrix}$$

Fig. 1: Temperature variation of tensor elements

When the temperature of the ferrite is increased - possibly due to either RF power or cooling water variation - the element values vary along the line B_{ext} = const. As a result, the operating point of the circulator is de-tuned. In order to obtain constant values of μ and κ, it can be seen that the external magnetization has to be changed by ΔB_{ext} (lines with μ, κ=const). The external variable magnetic field is generated by a combination of permanent and electromagnet, where the latter is used for fine tuning.

Field theoretical simulation of resonator geometry

Fig. 2 depicts a top and cross-sectional view of a typical ferrite-resonator geometry. The example is given for a design with four ferrite plates mounted on two metallic carriers.

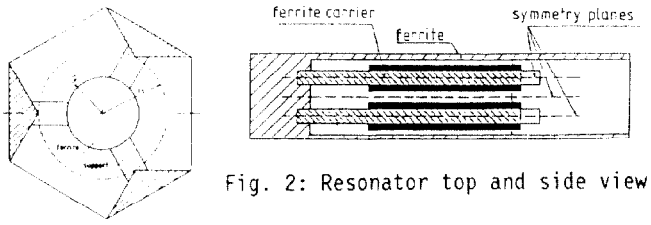

Fig. 2: Resonator top and side view

The term 'ferrite resonator' used in the following is understood as a self-contained cylindric cavity with a ground plane radius of r_1 and a height of h_r. The surface is assumed to be metallic. In order to simplify mode computation, the analysis of the cavity uses an 'elementary cell', which is shown in Fig.3.

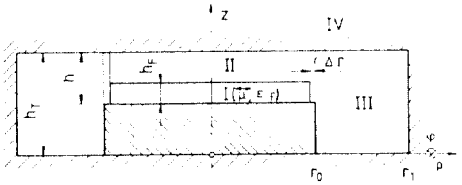

Fig. 3: Geometry of an elementary cell

The evaluation of resonance frequencies as well as electromagnetic field distribution may be done using the method of orthogonal series expansion. For this task, the elementary cell is divided into several segments(I...IV). The fields in each segment are then represented by an infinite set of discrete modes. For example: the z-component of the electric field in segment I or II has the following form written in equation (2):

$$E_{zm}^{I,II} = \left\{ \sum_{i=1}^{\infty} A_{mi} f_i(z)\, J_m(k_{ri}\varrho) \right\} e^{jm\varphi} \qquad (2)$$

The eigenvalues k_{ri} of the propagation constant as well as the function $f_i(z)$ are derived from continuity conditions at the boundary surface between region I and II. The outcome of the field-theoretical simulation is not only the field distribution inside the resonator - although very important for breakdown considerations - but also the behaviour of resonance frequencies depending on geometric parameters, which is a very powerful means for circulator design.
Fig. 4 presents a 'mode chart', where resonance frequencies are plotted versus ferrite resonator radii. The curves are graphs for the $EH_{\pm 110}$ modes with three different values of h_f/h_t (ferrite thickness / cell height). This chart may be used to select radius and other geometric values of the ferrite region for broad band operation, while bearing in mind the requirements of the thermal design (equation 1).

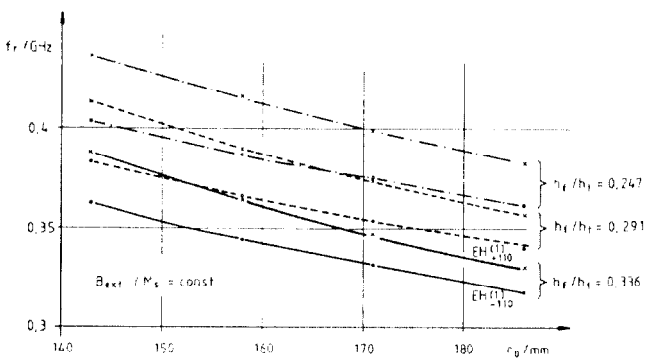

Fig. 4: Resonance frequencies vs. resonator radius for three different values of h_f/h_t

Scattering matrix considerations

Starting from resonator simulation, the next step is to match the electromagnetic resonator field to the H_{10} waveguide mode (more exactly: the H_{n0} modes, n=0...N) at $r=r_1$. This procedure, along with useful simplifications, is described in [4]. The admittance matrix of the coupled resonator is thus obtained, which can be transformed into the more useful scattering matrix $\underline{S}$ of a circulator. Typical s-parameter curves of a resonator junction are shown in Fig.5.

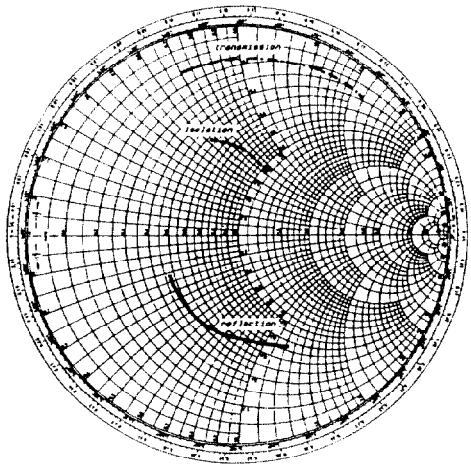

Fig. 5: Computed resonator s-parameters for the frequency range 332MHz to 372MHz

From network theory, it is a well-known fact that matching a symmetric three-port junction for optimum reflection loss (at all ports) results in a three-port circulator. Therefore the matching task can be reduced to a one-port impedance matching process.
Selecting matching elements must be effected very carefully, since in high-power operation the determining factors are the breakdown voltage of the electrical fields as well as the induced surface currents.

Measurement results

After optimization of impedance matching networks, the design process continues with the measurement of the small signal s-parameters. Up to this step, the whole design of the circulator has been derived from field-theoretical procedures, except for some slight modifications of the matching networks during the tuning process.

Small signal operation

The circulator behaviour was measured from 332MHz to 372MHz. The measurement method implies a HP8505-Network Analyzer, where s-parameters can be measured in the complex plane. The measurement ports of this analyzer are coaxial, so that coax-to-waveguide transitions (WR2300) have to be used. All errors resulting from the measurement setup are calibrated out by the well-known 12-term error correction procedure. In order to simplify calibration and transition handling, all measurements were effected at the coaxial reference plane. This means that the unknown measurement object consists of the circulator itself and three transitions. The frequency dependence of the transitions may then be extracted by a special de-embedding technique and thus the true s-matrix of the circulator can be derived. The following measurement results have been corrected in the described way (Fig. 6).

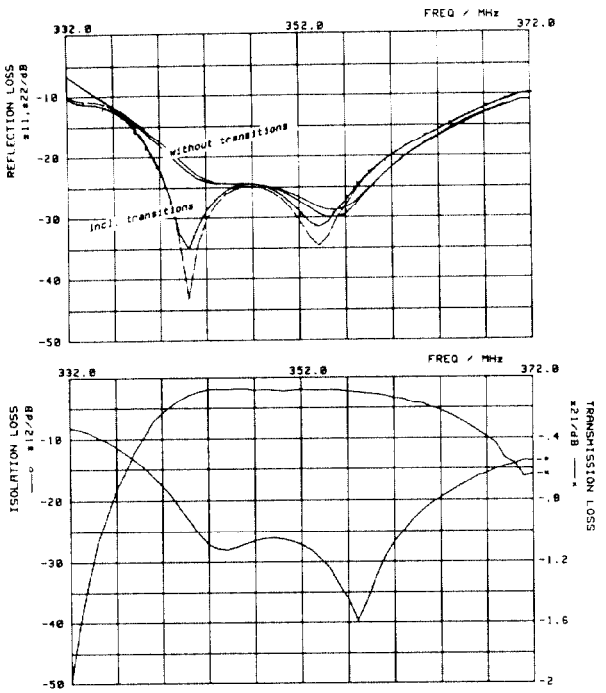

Fig.6: Small signal measurement results

Simulation of high-power s-matrix behaviour at small signal levels

The operational power level of the circulator is 1MW CW at 352MHz. As mentioned above, the ferrite material is sensitive to temperature. This factor has to be observed even at small signal levels. The mean temperature rise of the ferrites due to their losses is

$$\Delta T_0 = P_1[kW] \cdot 7 \cdot 10^{-3}\ °C \qquad (3)$$

at a forward power level of P_1 (with a water flow rate of 2200l/h). Thus, a high power simulation of s-parameters at small signal levels can be realized by simply changing the water input temperature to the corresponding value. For example: if the circulator is to be operated at a power level of 1MW with a cooling water input temperature of T_1=+24°C, the equivalent small signal simulation temperature (T_{ss}) is

$$T_{ss} = T_1 + \Delta T_0 = 31°C. \qquad (4)$$

High-power operation

For the LEP storage ring, the specifications for the circulator are as follows:

- mid-frequency: 352.2MHz
- forward power: 1100kW CW
- reverse power: 300kW CW (simultaneously applied, any phase)
- insertion loss: <0.15dB
- refl./isol. loss: ≥20dB (±3% bandwidth)
  ≥10dB (±5% bandwidth)

The power handling capability of the Y-junction circulator has been tested in pulsed mode (0.1% duty cycle) as well as in continuous wave (CW) mode. A good idea for effectively testing a Y-junction circulator is to use a measurement setup with a sliding short at the output of the circulator. If a specification with P_1=forward power and P_2=reverse power is given, then the equivalent forward power P1' when using a short at the output is:

$$P_1' = \tfrac{1}{4} \cdot (\sqrt{P_1} + \sqrt{P_2})^2 \qquad (5)$$

For example: P_1=1100kW, P_2=300kW --> P_1'=638kW.

This would be the equivalent circulator input power, with the circulator output shorted. The circulator design was tested up to a continuous wave input power of 1MW with the output still shorted: therefore, the equivalent forward power handling capacity is 4MW with a matched load at the output.
A comparison between phase-shift and Y-junction circulator shows, that the latter type can be operated over a wider power range than the first one. The reason for this behaviour may be explained from the fact, that a phase-shift circulator has distributed losses and thus the dissipation loss occuring when the output port is mismatched is simply the sum of forward and reverse power losses. Therefore -in contrast to eq. (5)- for a phase-shift circulator the sum of forward and reflected power is constant , whereas eq. (5) shows that the sum of the H-fields ($\sim\sqrt{P}$) is constant. This is due to the lumped losses of a Y-junction circulator.

Insertion loss

When examining a Y-junction circulator for ferrite losses and using a short circuit at the output port, great attention must be paid to the maximum dissipation power inside the ferrites. When operating at such special conditions, the maximum ferrite loss obtained is not simply twice the 'normal' insertion loss (operation with a load at the output) but three times the expected value [5]. Therefore, the maximum dissipation power of the LEP circulator is about 31kW. This is the worst case value for a forward power of 1MW with the output port shorted at worst phase. The minimum value is about 11kW. This means - for 'normal' operation into a matched load - that 11kW of the RF power is dissipated inside the ferrites, corresponding to an insertion loss of ≈0.04dB. Comparing this with small signal measurement results, it can be stated, that about half the value of the insertion loss is due to ferrite losses while the other half is due to waveguide and matching network losses.

Conclusion

As can be seen from the presentation given, this new Y-junction circulator is a really good replacement for phase-shift circulators, not only for reduced size and weight (1.6m x 1.9m ground plate, weight: 1.8t), but also for flexibility of electrical tuning and very low insertion losses. In the meantime, 17 circulators were manufactured and successfully tested at CERN/Geneva.

References

[1] E. Pivit, "Ein Hochleistungszirkulator für das deutsche Elektronen-Synchrotron DESY," Intern. Elektron. Rundschau, S. 101-103, April 1971.
[2] Y. Konishi, "A High-Power UHF Circulator," IEEE Trans. MTT, Vol. 15, No. 12, pp. 700-708, Dec. 1967.
[3] F. Okada, K. Ohwi, "Design of a High-Power CW Y-Junction Waveguide Circulator," IEEE Trans. MTT, Vol. 26, No. 5, pp. 364-369, May 1978.
[4] W. Hauth, S. Lenz, E. Pivit, "Entwurf und Realisierung von Hohlleiter-Verzweigungszirkulatoren für höchste Leistungen," FREQUENZ, Bd. 40, Nr. 1, S. 2-11, Januar 1986.
[5] J. Helszajn et al., "Insertion Loss of 3-Port Circulator with One Port Terminated in Variable Short Circuit," IEEE Trans. MTT, Vol. 23, No. 11, pp. 926-927, Nov. 1975.